Trends in Cancer Research
Vol. 16, 2021

Original Article

The advanced dose gradient index without the deficiencies of Paddick's dose gradient index

Markus Wösle*

Klinik für Strahlentherapie und Radioonkologie, Städtisches Klinikum Dessau, Dessau-Roßlau, Germany.

ABSTRACT

The ICRU Report 91 recommends, inter alia, Paddick's dose gradient index (*GI*) for reporting the values of dose gradients in stereotactic radiotherapy. Nevertheless, the *GI* shows false positive characteristics on a decreasing physical dose gradient $\nabla \cdot D$. One aim of ICRU Report 91 is to better associate treatment complications with the values of dose gradient indices. In this context, the *GI* is not suitable. Therefore, the author developed an advanced dose gradient index (*aGI*) to get rid of the deficiencies of the *GI*. A function of the volume product of the isodoses of interest was used to define the *aGI* instead of the volume ratio that defines the *GI*. The dose gradient distributions were quantified by the superficially averaged dose gradient (*SADG*). The values of the *SADG*, *aGI*, and *GI* were determined for the linac-based stereotactic radiosurgery and radiotherapy of 13 brain metastases and 25 choroidal melanomas, respectively. The *aGI* was proportional to $\Delta D/SADG$ with true characteristics in both irradiation series; ΔD = const. is the dose difference of the isodoses of interest. Pearson's correlation coefficients were $r \geq 0.647$. Contrary to the *aGI*, the *GI* showed false positive regression lines with $r \leq -0.511$. The growing *aGI* on a decreasing $|SADG|$ is reasonable because the *aGI* is nearly a reciprocal dose gradient measure in the form of a radius difference $\Delta r = \Delta D/\|\nabla \cdot D\|$. The utilisation of the *aGI* entails no limitations of the comparability of dose gradient values. The *GI* and other dose gradient indices based on volume ratios of the isodoses of interest should no longer be used for reporting dose gradient values.

KEYWORDS: advanced dose gradient index, reciprocal dose gradient measure, stereotactic radiotherapy, superficially averaged dose gradient, superficially averaged radius difference.

1. INTRODUCTION

The quality criteria in radiotherapy that specify the dose distribution within the target volume and at its boundary are the dose homogeneity, dose conformity, and irradiated volume. ICRU Report 62 and ICRU Report 83 recommend reporting the values of these parameters [1, 2]. The dose conformity characterises the degree to which the high dose region, appropriately modelled by the volume and surface of the prescribed isodose, conforms to the target volume.

Particularly in stereotactic radiotherapy and radiosurgery, clinical complications primarily occur due to the dose fall-off in a region between the surfaces of the prescribed isodose and another isodose defining the irradiated volume with an organ-specific tolerance dose level. In this regard, good dose conformity is one of the necessary conditions for the restriction of the absorbed dose to the normal tissue and organs at risk. Consequently, good dose conformity and steep dose gradients are necessary and sufficient conditions for sparing doses in healthy tissue.

The dose fall-off at the target volume's boundary can be characterised by different dose gradient

*Email ID: markus.woesle@klinikum-dessau.de

measures (in the literature, these were also designated as gradient indices or metrics). ICRU Report 91 recommends reporting one of two simple dose gradient metrics in addition to the conformity index [3]: the dose gradient index (*GI*) of Paddick *et al.* [4] or the volume of normal tissue irradiated with at least the dose D, V_D, for instance, $D = 12\ Gy$ for brain tissue [5, 6]. Nevertheless, both dose gradient metrics have shortcomings: The reporting of the *GI* per target volume is not realistic for treatment plans containing multiple targets with one common lower isodose surface because the numerator in its definition is oversized and the values become too large; the metric V_D is not suited for comparing quality between treatment plans for varying target volume sizes treated with different doses [3]. Further shortcomings of both dose gradient metrics were analysed and described in [7] and [8], respectively. Ohtakara *et al.* found false superior values of the *GI* in cases of prescribed isodoses that exaggerate the target volume's dose coverage [7]. Wösle showed that the metric $V_{12\ Gy}$ (*Brain*) underestimates physical dose gradients. Furthermore, the *GI* overvalues physical dose gradients with false positive curve characteristics on it. A cautionary clinical example demonstrated that a decrease in the physical dose gradient by the reduction factor 1/2.4 could not be detected by means of the *GI* because of indifferent values [8]. What has been just said about the serious deficiencies of the *GI* also applies to other dose gradient indices derived from the *GI*: the dose gradient (*DG*) of Akpati *et al.* [9] and the modified dose gradient index (*mGI*) of Ohtakara *et al.* [7].

Since 2000, several dose gradient measures have been defined and are clinically utilised. From a mathematical point of view, they are all one-dimensional and include

- single volumes of healthy tissue [5, 6],
- volume ratios of the isodoses of interest [4, 7, 10] or of healthy tissue under real and ideal irradiation conditions [11], respectively,
- radius differences between the isodoses of interest [12-14],
- dose difference quotients [15], or
- combinations of a dose gradient index with different indices, for example, for dose conformity [9, 16].

The first two-dimensional dose gradient measures were published in 2019 [8]. This comprehensive article moreover contains the definitions and explanations of 13 clinically utilised dose gradient measures. The particular informative content of 11 dose gradient measures was assessed by classification and analysing their properties. Two-dimensional dose gradient measures such as the superficially averaged dose gradient (*SADG*) best described clinical dose gradient distributions in an irradiation series for the linac-based stereotactic radiosurgery of 13 brain metastases. The reason is physical: in teletherapy with photon beams in humans, centrally symmetric dose distributions with isotropic dose gradient distributions are impossible. From all of the one-dimensional dose gradient measures, the spatially averaged dose gradient ($SADG^*$) showed the best correlation on the *SADG*. This one-dimensional approximation provides more information on the global anisotropic dose fall-off towards normal tissue and organs at risk than the *GI* [15].

All of the gradient measures aid in assessing treatment plans concerning clinical suitability and predicting the degree of severity of radiogenic side effects in critical structures. In this context, the quality of the description of a dose gradient problem is one necessary condition for the suitability of a one-dimensional dose gradient index for predicting normal tissue complication probabilities. The *GI*, *mGI*, and *DG* defined in [4, 7, 9] have the most severe shortcomings from all of the one-dimensional dose gradient indices:

1. They overestimate physical dose gradients what is reflected by false positive curve characteristics on the mean value of the physical dose gradients.
2. Their values are strongly dependent on the target volume size at a constant mean value of the physical dose gradients.
3. Indifferent values of the *GI*, *mGI*, and *DG* can occur even though the physical dose gradient considerably varies.
4. These dose gradient indices do not allow direct or approximate comparability of different patients and irradiation series concerning the dose gradients.

5. One important aim of the ICRU Report 91 is to better associate the treatment complications with the values of dose gradient indices *via* rigorous and uniform reporting of these parameters. The use of the *GI*, *mGI*, and *DG* makes this aim unattainable because of the items 1 to 3.
6. The use of these dose gradient indices regularly vexes medical physicists and radiation oncologists whenever multiple targets of different sizes must be irradiated: Why is the dose gradient of the larger target volume better than that of the smaller one, and vice versa?

To get rid of the aforementioned serious deficiencies of the *GI*, *mGI*, and *DG*, an advanced dose gradient index (*aGI*) was developed by the author. The present article will assess the new and the previous dose gradient indices by quantifying and comparing them with the values of two-dimensional dose gradient measures. All of the dose gradient measures were applied in two different linac-based irradiation series for the stereotactic radiosurgery of 13 globular brain metastases and for the stereotactic radiotherapy of 25 choroidal melanomas.

2. MATERIALS AND METHODS

2.1. Definitions of considered dose gradient measures

Wösle developed the first two-dimensional dose gradient measures that better describe anisotropic dose gradient distributions than all of the one-dimensional dose gradient indices. They are called the superficially averaged dose gradient (*SADG*) and the superficially averaged radius difference $\left(\overline{\Delta r}_{\Delta D}\right)$ between the isodoses of interest [8].

Both quantities yield reference values to investigate the quality of the assessed one-dimensional dose gradient indices in the present article. Its definitions are summarised and explained in Appendix A.1. The definitions of the herein analysed common one-dimensional dose gradient indices *GI*, *mGI*, and *DG* are contents of Subsection 2.2 and Appendix A.2, respectively.

2.2. Definition of and rationale to advanced dose gradient index

The definition of a completely new dose gradient measure without the deficiencies of the *GI*, called the advanced dose gradient index

$$aGI = \sqrt[6]{V_{PI(PTV)} \cdot V_{PI(PTV)/2}}\,, \tag{1}$$

is recommended to correct the false curve characteristics of the *GI*, *mGI,* and $DG \equiv GI^{-1}$ on the target volume size and the mean value of the physical dose gradients. The product in Eq. (1) contains the volumes encompassed by the prescription isodose *PI*(*PTV*) and half the prescription isodose *PI*(*PTV*)/2 at the boundary of the planning target volume (PTV).

The mathematical derivation of Eq. (1) becomes logical by analysing the definition

$$GI = \frac{V_{PI(PTV)/2}}{V_{PI(PTV)}} \tag{2}$$

of the *GI* [4]. The physical dose gradient magnitude at the planning target volume's boundary will disproportionately decline with the increasing target volume size because the physical penumbra of photon beams disproportionately increases with an increasing field size. Thus, the denominator in Eq. (2) grows faster than the numerator in this scenario. A false positive trend with a negative slope on a decreasing physical dose gradient magnitude is the mathematical consequence for the *GI*.

To obtain true trends, the volume $V_{PI\,(PTV)}$ acts as a "penalty factor" in Eq. (1). The *aGI* now grows with a decreasing dose gradient magnitude – as intended. The sixth root was applied to the volume product

- to reduce the *aGI* to 1 *cm*, which is nearly the same as other 1 *mm* or 1 *cm* reciprocal dose gradient measures, as well as
- to obtain approximately linear correlations on the mean value of the dose gradients.

Almost all of the treatment planning systems display volume values in the unit cm^3; consequently, the recommended unit of the *aGI* is *cm*.

The square root of the *aGI* in Eq. (1) was also evaluated because it showed stronger correlations

on the mean value of the physical dose gradients than the *aGI*. The corresponding regression functions were almost linear. This mathematical property gives the values of the dose gradient index $\sqrt{aGI}$ better qualitative and quantitative comparability with regard to the real dose gradients than it would be possible by the *aGI*.

2.3. Classification of dose gradient measures

The assessed dose gradient indices will be classified according to their mathematical and physical characteristics. The following classification describes similarities and distinguishing features of the dose gradient indices and helps explain the comparative results.

From a mathematical point of view, all of the dose gradient measures can be divided into three categories [8]:

I. Explicit,

II. inversely proportional, or

III. implicit.

These categories characterise the function type to describe the Euclidean norm $\|\nabla \cdot D(\boldsymbol{r})\|$ of the physical dose gradient at an arbitrary position $\boldsymbol{r}$ by a certain dose gradient measure [8].

Further classification criteria are the unit, the dimensionality, the flexibility in defining the levels of the isodoses of interest, the trend on an increasing magnitude of the dose gradient, the computational expense, the applicability to multiple target volumes, the presence of clinically validated correlations between complication rates and the values of a dose gradient measure, as well as the dependency of the value of a dose gradient measure on the target volume size.

2.4. Dependencies of dose gradient indices on target volume size at constant dose gradient

The dependencies of the *aGI* and the *GI* on the target volume size at a constant physical dose gradient at the target volume's boundaries were quantified by means of model calculations. Good dose gradient indices show weak or no dependencies.

For that purpose, some assumptions were made:

- The planning target volumes and the isodoses of interest are ideal spheres.
- The volume $V_{PI\,(PTV)}$ of the prescription isodose at the boundary of the planning target volume PTV is always identical to the planning target volume size V_{PTV}; both volumes have the radius $R_1 = \sqrt[3]{3 \cdot V_{PTV}/(4 \cdot \pi)}$ that is the independent variable of the model calculations. The radius of the second isodose of interest is $R_2 = \sqrt[3]{3 \cdot V_{PI(PTV)/2}/(4 \cdot \pi)}$.
- The dose difference between the levels of the isodoses of interest is constant. Hence, a constant physical dose gradient means a constant radius difference $\Delta R = R_2 - R_1 = \text{const.}$ between the isodoses of interest.

The definitions in Eqs. (1) and (2) can now be simplified to describe the wanted dependencies. The *aGI* as a function of R_1 is

$$aGI = \sqrt[6]{\left(\frac{4 \cdot \pi}{3}\right)^2 \cdot R_1^3 \cdot (\Delta R + R_1)^3}$$

$$= \sqrt[3]{\frac{4 \cdot \pi}{3}} \cdot \sqrt{R_1 \cdot (\Delta R + R_1)}$$

$$\Rightarrow \quad aGI \propto R_1 \,. \tag{3}$$

The result of Eq. (3) is an approximately direct proportionality between the *aGI* and the radius R_1 of the planning target volume. Otherwise, the *GI* as a function of R_1 is

$$GI = \frac{(\Delta R + R_1)^3}{R_1^3} = \left(\frac{\Delta R}{R_1} + 1\right)^3$$

$$\Rightarrow \quad GI \propto \frac{1}{R_1^3} \,. \tag{4}$$

Consequently, the *GI* is approximately in inverse proportion to R_1^3 and to the volume V_{PTV}.

2.5. Functions of dose gradient indices on dose gradient

The functions of the assessed dose gradient indices on the physical dose gradient aid in evaluating the quantitative description of changes in the physical dose gradient. Good dose gradient indices should show strong correlations with linear regression lines.

Similar to the model calculations in Subsection 2.4, some assumptions were made:

- The isodoses of interest are ideal spheres with the radii R_1 and R_2, like in Subsection 2.4.
- The dose difference between the levels of the isodoses of interest is constant. Hence, a decreasing absolute value of the physical dose gradient means a growing radius difference $\Delta R = R_2 - R_1$ between the isodoses of interest.
- The radius ratio R_2/R_1 on the variable R_1 remains almost constant in stereotactic treatments with small photon beams in case of unchanged photon energy and tumour centre-to-skin distance. Consequently, the constant $c = R_2/R_1$ was introduced to specify the wanted functions.

The radius difference as a dose gradient measure can now be written in the form

$$\Delta R = c \cdot R_1 - R_1 = (c-1) \cdot R_1$$

$$\Leftrightarrow \quad R_1 = \frac{1}{c-1} \cdot \Delta R\,. \tag{5}$$

The wanted functions are obtained by introducing R_1, R_2, and c as well as substituting Eq. (5) into Eq. (1) and Eq. (2):

$$aGI = \sqrt[3]{\frac{4 \cdot \pi}{3}} \cdot \sqrt{R_1 \cdot R_2} = \sqrt[3]{\frac{4 \cdot \pi}{3}} \cdot \sqrt{c} \cdot R_1$$

$$= \sqrt[3]{\frac{4 \cdot \pi}{3}} \cdot \frac{\sqrt{c}}{c-1} \cdot \Delta R \quad \Rightarrow \quad aGI \propto \Delta R\,, \tag{6}$$

$$GI = \frac{(c \cdot R_1)^3}{R_1^3} = c^3 \quad \Rightarrow \quad GI = \text{const.} \tag{7}$$

Therefore, the *aGI* is directly proportional to the dose gradient measure ΔR, and the *GI* is a constant with indifferent values on the variable ΔR.

2.6. Plausibility check of trends in dose gradient measures

Trends in dose gradient measures will be compared with measured dose difference quotients within the penumbra according to IEC 60976 [17]. The beam collimation on a Novalis powered by TrueBeam™ STx (Varian Medical Systems, Inc., Palo Alto, CA, USA) was achieved by circular cones (Brainlab AG, Munich, Germany). A diode E 60017 (PTW GmbH, Freiburg, Germany) was used for the measurements in water.

2.7. Statistics

Pearson's correlation coefficient r was used to quantify the strength of a correlation. The probabilities p of zero correlation were calculated using a one-sided association test based on Student's t test with n-2 degrees of freedom, where n is the sample size. A significance level of $\alpha = 0.05$ was used and all confidence levels were $1 - \alpha = 0.95 \mathrel{\widehat{=}} 95\%$. The quality of estimating a correlation by a regression function was evaluated using the coefficient of determination r^2 [18].

2.8. Treatment and calculation parameters

The possible correlations of the examined dose gradient indices on the mean value of the physical dose gradients were investigated in two irradiation series. The author used the treatment planning system iPlan® RT Dose 4.5.3 and 4.5.5 (Brainlab AG, Munich, Germany). The irradiation machine was a Novalis powered by TrueBeam™ STx with a dynamic multi-leaf collimator HD 120™ (Varian Medical Systems, Inc., Palo Alto, CA, USA). The dose fractions were applied by 5.6 *MV* flattening filter-free photons with dose rates in a range of 800 to 1 400 *MU/min* (*MU* – monitor unit).

2.8.1. Stereotactic radiosugery for brain metastases

Firstly, the values of all of the considered dose gradient measures were calculated for the virtual irradiations of 13 spherical brain metastases treated with one single-dose fraction and marginal dose values in a range of 18 to 25 *Gy*. All of the dose prescriptions strictly complied with the recommendations of the DEGRO Working Group on Stereotactic Radiotherapy [19]. The planning target volume diameters were systematically varied in a range of 3 to 29 *mm* to achieve steadily decreasing nearly isotropic dose gradients on this variable.

Linac-based stereotactic radiosurgery of 13 brain metastases with a median planning target volume

size of 1.60 cm^3 (range 0.01-12.77 cm^3) was planned. All of the planning target volumes were segmented in the left temporo-parietal hemisphere on the cranial computer tomographs of one patient without lesions. The uniform distance of the geometrical centre of mass of all of the target volumes to the skin was 35 *mm*. An additional isotropic margin of 0.5 *mm* was chosen between the planning target volume and the irradiation field aperture. The gantry arc lengths with circular cones for the diameter range of 3 to 14 *mm* were $\Delta G = 150^{\circ} = \text{const.}$ and applied together with five different couch angles with the angle increment $\Delta T = 30^{\circ} = \text{const.}$ The irradiations by dynamic conformal arcs with a high-definition multi-leaf collimator at the diameter range of 14 to 29 *mm* were performed by the gantry arc lengths $\Delta G = 130^{\circ} = \text{const.}$ The couch angles were the same as previously mentioned. The beam geometry minimised the anisotropy of the radii of the isodoses of interest.

For comparability, the same levels of the isodoses of interest were used for the calculation of all of the dose gradient measures: 80% and 40% of the individual maximum dose within the planning target volume. Marginal isodose levels in a range of 60 to 80% ensure steepest possible dose gradients [19]. The author chose the isodose level 80% to define the treated volume and the usually used isodose at halved level for the definition of the irradiated volume.

2.8.2. Stereotactic radiotherapy for choroidal melanomas

Secondly, the values of all of the considered dose gradient measures were also determined for the clinically realised treatments of 25 malignant choroidal melanomas treated with 50 *Gy* in five fractions.

Linac-based stereotactic radiotherapy of 25 irregularly formed choroidal melanomas with a median planning target volume size of 1.84 cm^3 (range 0.42-3.37 cm^3) was planned. The dose optimisation and calculation for the irradiation technique HybridArc™ (Brainlab AG, Munich, Germany) were performed; for details, see [15].

For comparability, the same isodoses of interest were used for the calculation of all of the dose gradient measures: The upper isodose level at the boundary of the planning target volume was always 86% and the lower isodose level was 43% of the prescribed tumour dose 50 *Gy*. The dose level 86% was the mean value of the minimum dose values of all of the planning target volumes and defined the treated volumes. Furthermore, the distal isodose of interest at halved level is also used in the definitions of the common dose gradient indices.

3. RESULTS

3.1. Mathematical evidence of evolution from *GI* to *aGI*

Here, the author will present the mathematical properties of the ratio and functions of the product of the volumes of the isodoses of interest and its impacts on the corresponding dose gradient indices *GI* and *aGI*, respectively.

Figure 1 shows the trends of the volumes of interest on the diameter d_{PTV} of the planning target volume for the stereotactic radiosurgery of 13 globular brain metastases. The first three data rows of Table 1 contain the parameters of the related regression functions. Power functions adequately describe the regressions with r^2 in a range of 0.999 to 1.000. Their exponents to describe the aforementioned trends in the planning target volume and in the volume of the isodose at level $D_1 = 80\%$ were $b \geq 3.000$. They were larger than the exponents for the volume of the isodose at level $D_2 = 40\%$, whereby $b \leq 2.667$ for the lesions treated by the circular cones and multi-leaf collimator.

As a result of the application of the power laws, the volume ratios could also adequately be described by means of power functions with exponents $b < 0$ for the *GI* as well as *mGI* and $b > 0$ for the *DG*. On the other hand, the *aGI* is a function of the product of the volumes of interest that grew on an increasing target volume size and on a decreasing magnitude of the physical dose gradient with $b > 0$. For more details, see Table 1.

3.2. Dependencies of dose gradient indices on target volume size at constant dose gradient

An important property of a dose gradient index is its dependency on the target volume size, whereby the dose gradient is a constant. A strong dependence

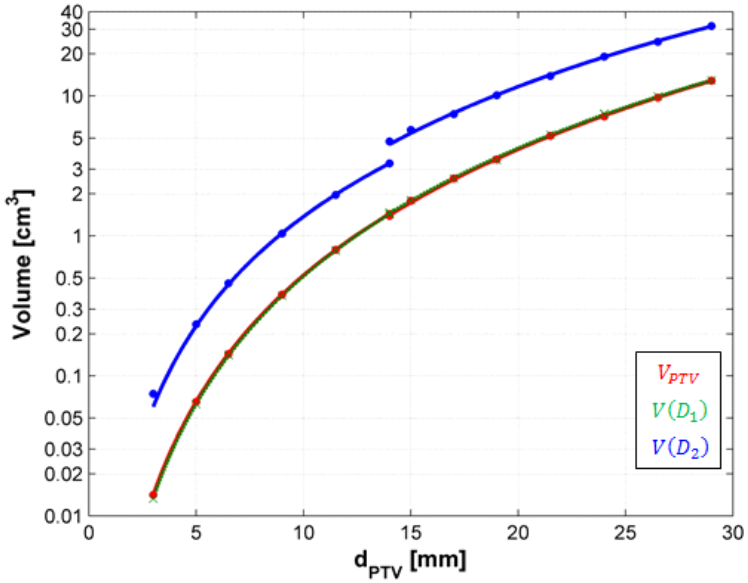

Figure 1. Volumes of interest as functions of the planning target volume diameter d_{PTV} for the stereotactic radiosurgery of 13 brain metastases; the scale of the ordinate is logarithmic. V_{PTV} - planning target volume size; $V(D_1)$ - volume of the isodose at level D_1 = 80% relative to the maximum dose; $V(D_2)$ - volume of the isodose at level D_2 = 40%.

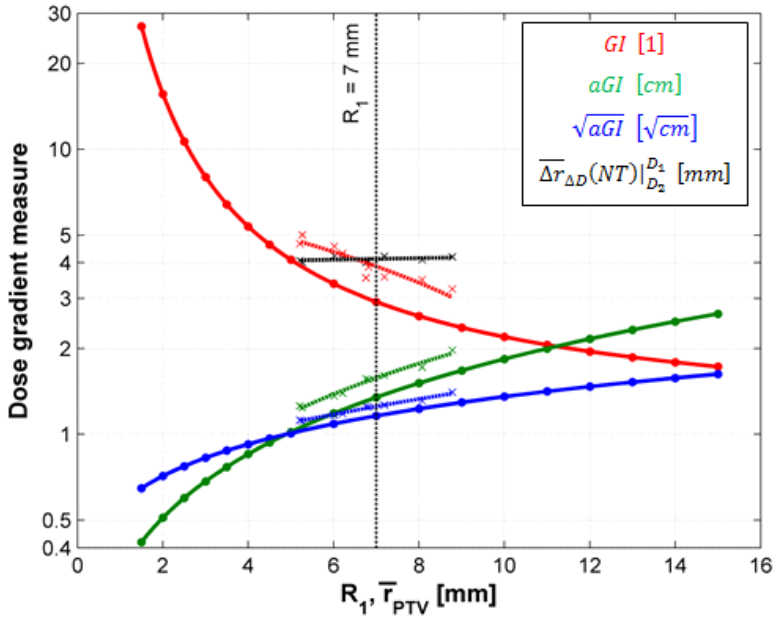

Figure 2. Dependencies of dose gradient measures on the target volume radius in a model calculation (solid lines with circular markers) and for the stereotactic radiotherapy of nine choroidal melanomas (dashed lines with crosses); the scale of the ordinate is logarithmic. R_1 - radius of the spherical target volume; $\overline{r}_{PTV}$ - superficially averaged radius of the planning target volume PTV; *GI* - dose gradient index according to Eq. (2); *aGI* - advanced dose gradient index according to Eq. (1); $\sqrt{aGI}$ - square root of the *aGI*; $\overline{\Delta r}_{\Delta D}(NT)\big|_{D_2}^{D_1}$ - superficially averaged radius difference between the isodoses of interest at levels D_1 = 86% and D_2 = 43% of the nominal tumour dose 50 *Gy*.

Table 1. Regression parameters of volumes of interest, two-dimensional dose gradient measures, and one-dimensional dose gradient indices on the planning target volume diameter for the stereotactic radiosurgery of 13 brain metastases. $x = d_{PTV}$ - diameter of the planning target volume; $f(x) = a \cdot x^b$ - regression power function; a - coefficient of the power function; b - exponent of the power function; X and Y - different units so that $a \cdot x^b$ has the unit of the corresponding quantity; r^2 - coefficient of determination; V_{PTV} - planning target volume size; $V(D_1)$ - volume of the isodose of interest at level D_1 = 80% of the maximum dose; $V(D_2)$ - volume of the isodose of interest at level D_2 = 40%; $|SADG(NT)|_{D_2}^{D_1}|$ - absolute value of the superficially averaged dose gradient for nonspecific normal tissue (NT) according to Eq. (A.1) between the isodoses at levels D_1 and D_2; $\overline{\Delta r}_{\Delta D}(NT)|_{40\%}^{80\%}$ - superficially averaged radius difference for nonspecific normal tissue according to Eq. (A.2) between the isodoses at levels D_1 and D_2; *GI* - dose gradient index according to Eq. (2); *DG* - dose gradient according to Eq. (A.8); *mGI* - modified dose gradient index according to Eq. (A.3); *aGI* - advanced dose gradient index according to Eq. (1); $\sqrt{aGI}$ - square root of the *aGI*.

Collimation type	**Circular cones**			**Multi-leaf collimator**		
Volume/dose gradient measure	a [X]	b [Y]	r^2 [1]	a [X]	b [Y]	r^2 [1]
V_{PTV} [cm^3]	$5.236 \cdot 10^{-4}$	3.000	1.000	$4.668 \cdot 10^{-4}$	3.035	1.000
$V(D_1)$ [cm^3]	$4.764 \cdot 10^{-4}$	3.035	1.000	$5.152 \cdot 10^{-4}$	3.009	1.000
$V(D_2)$ [cm^3]	$3.480 \cdot 10^{-3}$	2.597	1.000	$3.957 \cdot 10^{-3}$	2.667	0.999
$\lvert SADG(NT)\rvert_{D_2}^{D_1}\rvert$ [%/mm]	54.196	-0.408	0.987	44.953	-0.502	0.974
$\overline{\Delta r}_{\Delta D}(NT)\rvert_{D_2}^{D_1}$ [mm]	0.680	0.445	0.997	0.822	0.527	0.981
GI [1]	10.636	-0.610	0.979	9.477	-0.409	0.965
DG [1]	0.111	0.524	0.984	0.109	0.398	0.963
mGI [1]	9.535	-0.567	0.978	10.268	-0.430	0.942
aGI [*cm*]	0.112	0.928	1.000	0.115	0.940	1.000
$\sqrt{aGI}$ [$\sqrt{cm}$]	0.336	0.462	1.000	0.340	0.469	0.999

may entail either false positive or false negative dose gradient values. The results of the model calculations specified in Subsection 2.4 will now be presented.

Figure 2 shows the functions of the dose gradient indices *GI*, *aGI*, and $\sqrt{aGI}$ on the radius R_1 of the spherical planning target volume. The radius difference between the isodoses of interest is a reciprocal dose gradient and was ΔR = 3 *mm* = const. As a result, the analytical functions were fractional rational or irrational algebraic, according to Eqs. (4) and (3), respectively:

$$GI(R_1) = \left(\frac{3\ mm}{R_1} + 1\right)^3 ;$$

$$aGI(R_1) = 0.161 \cdot \sqrt{R_1 \cdot (R_1 + 3\ mm)}\ \ [cm] .$$

The results for the *DG* and *mGI* were not presented in Figure 2 because they are mathematically related to the results for the *GI* by $DG \equiv GI^1$ and $mGI \equiv GI$.

The ratios of the maximal to minimal functional index values on the definition range $R_1 \in [1.5, 15.0]\ mm$ were 15.6, 15.6, 6.3, and 2.5 for the *GI*, *DG*, *aGI*, and $\sqrt{aGI}$. For the four dose gradient indices, the percentage deviations of the functional values to the functional value at R_1 = 7 *mm* were in ranges of -40.7 to 826.1%, -89.2 to 68.7%, -68.9 to 96.4%, and -44.3 to 40.1%, respectively. The values of the derivatives $dX/dR_1|_{R_1 = 7\ mm}$ with $X \in \{GI, DG, aGI, \sqrt{aGI}\}$ were -0.375 mm^{-1}, 0.044 mm^{-1}, 0.164 *cm*/*mm*, and $0.071\ \sqrt{cm}/mm$, respectively.

3.3. Functions of dose gradient indices on dose gradient

A good dose gradient index should be directly proportional to the physical dose gradient. The results of the model calculations specified in Subsection 2.5 will now be presented.

Figure 3 summarises the functional relations between the dose gradient indices *GI*, *aGI*, and $\sqrt{aGI}$ on the radius difference $\Delta R = R_2 - R_1 \in [0.8, 7.5]\ mm$ between the isodoses of interest; ΔR is the reciprocal dose gradient. For this, one assumption was that the ratio of the radii of the spherical isodoses of interest is the constant $c = R_2/R_1 = 1.5$.

As a result, the *GI* was independent of the dose gradient with $GI(\Delta R) = 3.375 = \text{const.}$ according to Eq. (7). In contrast, the *aGI* was directly proportional to ΔR with the proportionality factor 0.395 *cm/mm* according to Eq. (6). The square root of the *aGI* obeyed the function $\sqrt{aGI} = 0.628\ \sqrt{cm/mm} \cdot \sqrt{\Delta R}$.

The results for the *DG* and *mGI* were not presented in Figure 3 because they are mathematically related to the results for the *GI* by $DG \equiv GI^{-1}$ and $mGI \equiv GI$ assuming that $V_{PTV} = V(D_1)$; see also Subsection 2.4. Therefore, they are also indifferent dose gradient indices.

Figure 4 presents the radius ratios of the volumes of interest for both irradiation series to demonstrate that the assumption for *c* is profound and *c* is at least approximately constant. The clinical isodoses at levels D_1 and D_2 were not ball-shaped. As a consequence, the calculation of their radii could not be analytically performed, but the radii of interest $\bar{r}_1 = \bar{r}(D_1)$ and $\bar{r}_2 = \bar{r}(D_2)$ were superficially averaged analogously to the integral in Eq. (A.1).

The values of the real radius ratio *c** were in ranges of 1.322 to 1.784 and 1.345 to 1.477 for the lesions treated by the circular cones and by the multi-leaf collimator, respectively, in the first irradiation series. The corresponding range in the second irradiation series was 1.466 to 1.829. The nonlinear regression function of *c** on $\bar{r}_1$ was $c^*(\bar{r}_1) = 1.887 \cdot \bar{r}_1^{-0.193}$ for the lesions treated by the circular cones. On the other hand, the corresponding regression lines obeyed the functions $c^*(\bar{r}_1) = -0.018 \cdot \bar{r}_1 + 1.598$ and $c^*(\bar{r}_1) = -0.054 \cdot \bar{r}_1 + 2.031$ for the lesions treated by the multi-leaf collimator in the first and second irradiation series, respectively. All of the coefficients of determination were $r^2 \in \{0.980, 0.941, 0.872\}$.

3.4. Curve characteristics of dose gradient measures on target volume size

This section presents the qualities of the investigated dose gradient indices *GI*, *DG*, *mGI*, and *aGI* in the quantification of the physical dose gradients for the stereotactic radiosurgery of the brain metastases. The mean value of the physical dose gradients will be described by the two-dimensional dose gradient measures *SADG* and $\overline{\Delta r}_{\Delta D}$.

Figure 5 shows the trends and nonlinear regression functions for all of the aforementioned dose gradient measures on the diameter d_{PTV} of the planning target volume. The smaller lesions with $d_{PTV} \leq 14\ mm$ were treated with circular cones, and the larger with $d_{PTV} \geq 14\ mm$ were treated with the multi-leaf collimator. Table 1 summarises the coefficients and exponents of the power functions that adequately describe the regressions of the dose gradient measures with r^2 in a range of 0.942 to 1.000.

The characteristics of $\left|SADG(NT)\right|_{D_2}^{D_1}\right|$ represent the particular under-proportionately decreasing absolute values of the physical dose gradient with the exponents $b \in \{-0.408, -0.502\}$ on an increasing field size formed by the circular cones and multi-leaf collimator, respectively. The just described trend is physically plausible, as seen from a comparison with the orange graph in Figure 5 that is an extract from the utilised linac's basic data. It presents the quantitative decrease of the absolute value of the dose difference quotient $\left|\Delta D/\Delta r\right|_{20\%}^{80\%}\right|$ within the radially symmetric penumbra on the diameter $x = d_{Cone}$ of the circular cone. The corresponding nonlinear regression function $f(x) = 74.949 \cdot x^{-1.311} + 34.744$ is adequate with $r^2 = 0.996$. The trends in $\left|SADG(NT)\right|_{D_2}^{D_1}\right|$ on d_{PTV} and the trends in $\left|\Delta D/\Delta r\right|_{20\%}^{80\%}\right|$ on d_{Cone} are qualitatively equal.

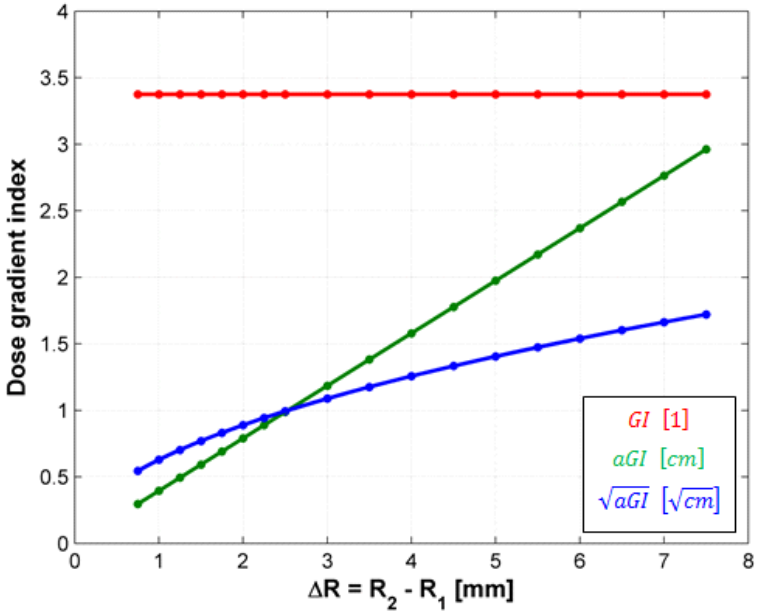

Figure 3. Dependencies of dose gradient indices on the physical dose gradient in a model calculation. R_1 - radius of the spherical isodose of interest at an arbitrary level D_1; R_2 - radius of the spherical isodose of interest at an arbitrary level $D_2 < D_1$; ΔR - radius difference between both isodoses is the reciprocal dose gradient in the model; *GI* - dose gradient index according to Eq. (2); *aGI* - advanced dose gradient index according to Eq. (1); $\sqrt{aGI}$ - square root of the *aGI*.

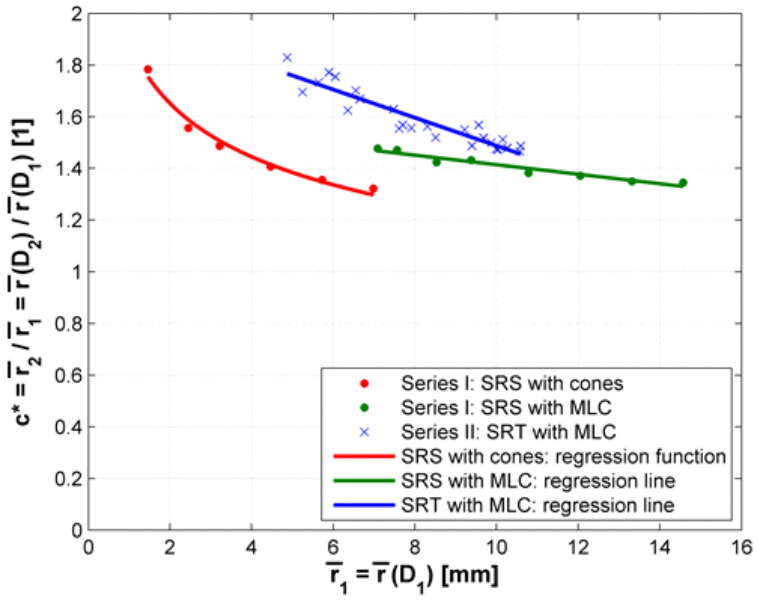

Figure 4. Dependencies of the radius ratio c^* on the radius of the proximal isodose of interest for the stereotactic radiosurgery (SRS) of 13 brain metastases (series I) and stereotactic radiotherapy (SRT) of 25 choroidal melanomas (series II). $\bar{r}_1 = \bar{r}(D_1)$ - superficially averaged radius of the isodose at level D_1 calculated analogously to Eq. (A.1); $\bar{r}_2 = \bar{r}(D_2)$ - superficially averaged radius of the isodose at level D_2; $D_1 = 80\%$ and $D_2 = 40\%$ of the maximum dose in series I; $D_1 = 86\%$ and $D_2 = 43\%$ of the nominal tumour dose in series II; *MLC* - multi-leaf collimator.

According to Eq. (A.2), the superficially averaged radius difference $\overline{\Delta r}_{\Delta D}(NT)|_{D_2}^{D_1}$ is inversely proportional to $|SADG\,(NT)|_{D_2}^{D_1}|$. As a result, the exponents $b \in \{0.445, 0.527\}$ of its regression functions showed changes of sign; additionally, the increase of $\overline{\Delta r}_{\Delta D}(NT)|_{D_2}^{D_1}$ was less than proportional on a growing d_{PTV}.

The *GI* followed power functions with the exponents $b \in \{-0.610, -0.409\}$. The negative exponents are the result of the definition in Eq. (2) with the power functions of $V(D_2)$ and $V(D_1)$. For both collimation types, the differences between the isodose volumes' exponents became negative and were approximately equal to the exponents of the *GI*. The exponents $b \in \{-0.567, -0.430\}$ of the regression functions for the *mGI* were roughly equal to those for the *GI* because $V_{PTV} \approx V(D_1)$. The exponents $b \in \{0.524, 0.398\}$ for the *DG* showed changes of sign compared to the exponents for the *GI* because $DG \equiv GI^{-1}$.

According to Table 1, the *aGI* could be approximately described by increasing lines because the exponents were $b \in \{0.928, 0.940\}$ for the circular cones and multi-leaf collimator, respectively. The *aGI* grew on a decreasing magnitude of the physical dose gradient.

An ideal dose gradient index would exactly describe relative variations of the physical dose gradient. In this regard, the *aGI* seems not to be ideal because its exponents differ by a factor of approximately 2 from those of $\overline{\Delta r}_{\Delta D}(NT)|_{D_2}^{D_1}$. Therefore, the characteristics of the ideal dose gradient index should be power functions with the exponents $b \in \{0.445, 0.527\}$ of $\overline{\Delta r}_{\Delta D}(NT)|_{D_2}^{D_1}$ for the irradiations through the circular cones and multi-leaf collimator, respectively. The exponents of the regression functions for the *aGI* were 108.5% and 78.5% larger than the ideal values for both collimation types (see Table 1). Consequently, the author also calculated the exponents for $\sqrt{aGI}$: $b \in \{0.462, 0.469\}$. They were merely 3.7% larger and -11.0% smaller, respectively, than the ideal values. Figure 5 shows the disproportionately low increasing characteristics of $\sqrt{aGI}$ on a growing d_{PTV}.

3.5. Correlation analyses between dose gradient measures

The superficially averaged radius difference $\overline{\Delta r}_{\Delta D}(NT)|_{D_2}^{D_1}$ was picked out to be the reference variable for the correlation analyses between the dose gradient measures. The objective of these analyses is to grade the dose gradient indices by their strengths of correlation on the mean value of the physical dose gradients.

3.5.1. Stereotactic radiosurgery for brain metastases

The correlations and regression lines of the assessed dose gradient indices and the values of Pearson's correlation coefficient *r* for the stereotactic radiosurgery of the brain metastases are presented in Figure 6 and Table 2.

The new advanced dose gradient index *aGI* showed the strongest correlations on $x = \overline{\Delta r}_{\Delta D}(NT)|_{D_2}^{D_1}$ with $r \geq 0.991$ and $p \leq 1.8 \cdot 10^{-5}$ for both collimation types. The corresponding values of the *GI*, *DG*, and *mGI* were in ranges of $0.911 \leq |r| \leq 0.987$ and $2.3 \cdot 10^{-4} \leq p \leq 1.1 \cdot 10^{-2}$.

The regression lines for the *aGI* obeyed the functions $f(x) = 0.907\ cm/mm \cdot x - 0.746\ cm$ and $f(x) = 0.859\ cm/mm \cdot x + 0.984\ cm$ for the lesions treated by the circular cones and multi-leaf collimator, respectively. The corresponding regression functions for $\sqrt{aGI}$ were $f(x) = 0.530\ \sqrt{cm}/mm \cdot x - 0.031\ \sqrt{cm}$ and $f(x) = 0.340\ \sqrt{cm}/mm \cdot x + 0.173\ \sqrt{cm}$, respectively.

3.5.2. Stereotactic radiotherapy for choroidal melanomas

The correlation parameters and regression lines of the assessed dose gradient indices for the stereotactic radiotherapy of the choroidal melanomas are summarised in Figure 7 and Table 3.

The new advanced dose gradient index *aGI* together with $\sqrt{aGI}$ showed the strongest correlations on $x = \overline{\Delta r}_{\Delta D}(NT)|_{D_2}^{D_1}$ with $r \geq 0.647$ and $p \leq 4.7 \cdot 10^{-4}$. The corresponding values of the *GI*, *DG*, and *mGI* were in ranges of $0.444 \leq |r| \leq 0.511$ and $9.0 \cdot 10^{-3} \leq p \leq 2.6 \cdot 10^{-2}$. The standard deviations *s* in the *GI* and *mGI* were

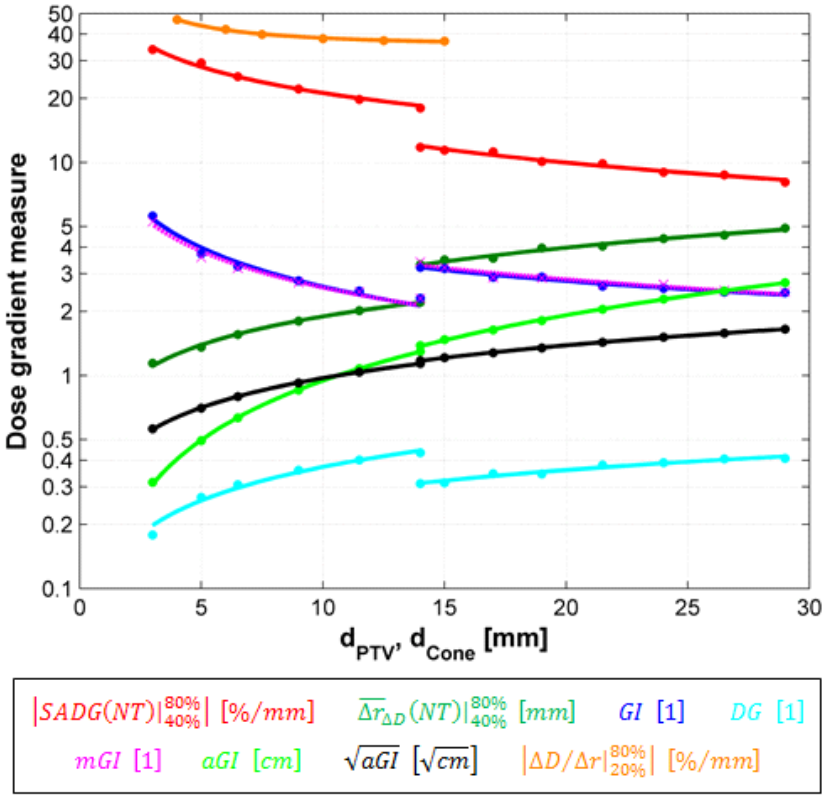

Figure 5. Dose gradient measures as functions of the planning target volume diameter d_{PTV} for the stereotactic radiosurgery of 13 brain metastases and as a function of the circular cone diameter d_{Cone} in measurements, respectively; the scale of the ordinate is logarithmic. The flattening filter-free photon energy was 5.6 *MV*, the source-to-phantom distance was 92.5 *cm*, and the detector depth was 75 *mm* during the measurements in water. $|SADG(NT)|_{40\%}^{80\%}|$ - absolute value of the superficially averaged dose gradient for nonspecific normal tissue (NT) according to Eq. (A.1) between the isodoses at levels 80 and 40% relative to the maximum dose; $\overline{\Delta r}(NT)|_{40\%}^{80\%}$ - superficially averaged radius difference for nonspecific normal tissue according to Eq. (A.2) between the same isodoses of interest; *GI* - dose gradient index according to Eq. (2); *DG* - dose gradient according to Eq. (A.8); *mGI* - modified dose gradient index according to Eq. (A.3); *aGI* - advanced dose gradient index according to Eq. (1); $\sqrt{aGI}$ - square root of the *aGI*; $|\Delta D/\Delta r|_{20\%}^{80\%}|$ - absolute value of the dose difference quotient within the penumbra between the dose levels 20 and 80% relative to the central axis intensity.

0.7 and 0.9, respectively, and thus remarkably larger than the corresponding values $s \leq 0.3$ in the other dose gradient indices; see Figure 7. The regression lines for the *aGI* and $\sqrt{aGI}$ obeyed the functions $f(x) = 0.593\ cm/mm \cdot x - 0.873\ cm$ and $f(x) = 0.241\ \sqrt{cm}/mm \cdot x + 0.255\ \sqrt{cm}$, respectively.

The dependencies of the *aGI* and $\sqrt{aGI}$ on the superficially averaged radius $x = \bar{r}_{PTV}$ of the planning target volume were analysed for the stereotactic radiotherapy of nine choroidal melanomas with approximately constant physical dose gradients; $\overline{\Delta r}_{\Delta D}(NT)|_{D_2}^{D_1}$ was in a range of 4.0 to 4.2 *mm* with a median of 4.1 *mm* and a standard deviation of $s < 0.1$ *mm*. The regression lines for the *GI*, *aGI*, and $\sqrt{aGI}$ obeyed the functions $f(x) = -0.481\ mm^{-1} \cdot x + 7.25$ with $r^2 = 0.848$, $f(x) = 0.194\ cm/mm \cdot x + 0.217\ cm$ with $r^2 = 0.975$, and $f(x) = 0.077\ \sqrt{cm}/mm \cdot x + 0.707\ \sqrt{cm}$ with $r^2 = 0.979$, respectively. The regression line for the physical dose gradient was nearly a constant function with a slope of $f'(x) = 0.024$.

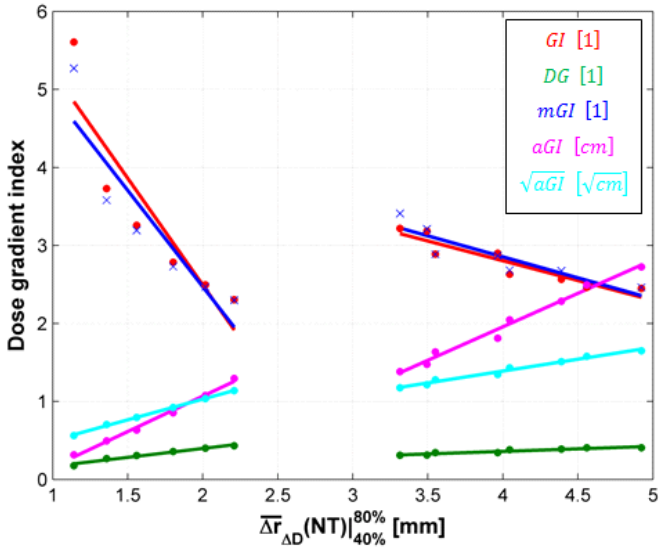

Figure 6. Correlations with regression lines of dose gradient indices on the physical dose gradient for the stereotactic radiosurgery of 13 brain metastases. $\overline{\Delta r}(NT)|_{40\%}^{80\%}$ - superficially averaged radius difference for nonspecific normal tissue (NT) according to Eq. (A.2) between the isodoses at levels 80 and 40% relative to the maximum dose; *GI* - dose gradient index according to Eq. (2); *DG* - dose gradient according to Eq. (A.8); *mGI* - modified dose gradient index according to Eq. (A.3); *aGI* - advanced dose gradient index according to Eq. (1); $\sqrt{aGI}$ - square root of the *aGI*.

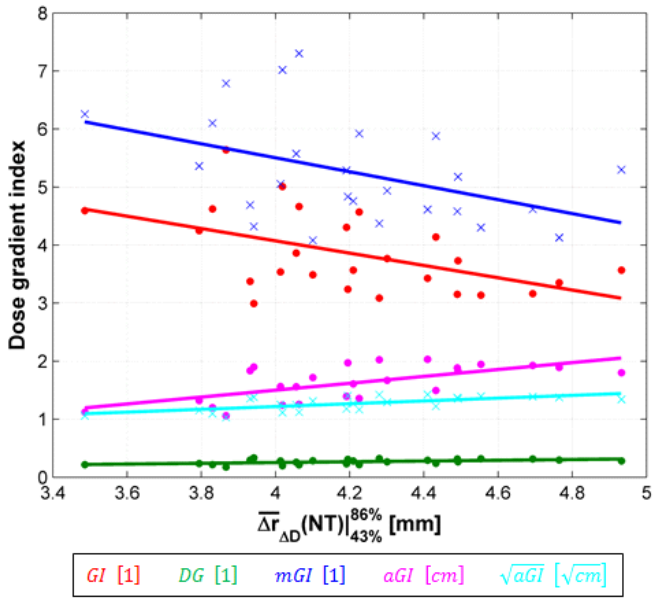

Figure 7. Correlations with regression lines of dose gradient indices on the physical dose gradient for the stereotactic radiotherapy of 25 choroidal melanomas. $\overline{\Delta r}(NT)|_{43\%}^{86\%}$ - superficially averaged radius difference for nonspecific normal tissue (NT) according to Eq. (A.2) between the isodoses at levels 86 and 43% relative to the nominal tumour dose 50 *Gy*; *GI* - dose gradient index according to Eq. (2); *DG* - dose gradient according to Eq. (A.8); *mGI* - modified dose gradient index according to Eq. (A.3); *aGI* - advanced dose gradient index according to Eq. (1); $\sqrt{aGI}$ - square root of the *aGI*.

Table 2. Correlation parameters of dose gradient indices on the superficially averaged radius difference $\overline{\Delta r}_{\Delta D}(NT)\big|_{D_2}^{D_1}$ for nonspecific normal tissue (NT) according to Eq. (A.2) for the stereotactic radiosurgery of 13 brain metastases. *r* - Pearson's correlation coefficient; *p* probability of zero correlation; $\|\nabla \cdot D(\boldsymbol{r})\| \nearrow$ - increasing dose gradient magnitude; D_1 = 80% - level of the proximal isodose of interest relative to the maximum dose; D_2 = 40% - level of the distal isodose of interest; ↗ - increasing dose gradient index; ↘ - decreasing dose gradient index; *GI* - dose gradient index according to Eq. (2); *DG* - dose gradient according to Eq. (A.8); *mGI* - modified dose gradient index according to Eq. (A.3); *aGI* - advanced dose gradient index according to Eq. (1); $\sqrt{aGI}$ - square root of the *aGI*. [a]Or the equivalent trend on $\overline{\Delta r}_{\Delta D}(NT)\big|_{D_2}^{D_1}$ ↘. [b]False trend compared to the intention of the dose gradient metric's authors.

Collimation type	**Circular cones**		**Multi-leaf collimator**		**Both**
Dose gradient index	***r* [1]**	***p* [1]**	***r* [1]**	***p* [1]**	**Trend on $\|\nabla \cdot D(\boldsymbol{r})\| \nearrow$ [a]**
GI	-0.911	$1.1 \cdot 10^{-2}$	-0.931	$7.6 \cdot 10^{-4}$	↗ [b]
DG	0.987	$2.3 \cdot 10^{-4}$	0.944	$4.1 \cdot 10^{-4}$	↘ [b]
mGI	-0.914	$1.1 \cdot 10^{-2}$	-0.917	$1.3 \cdot 10^{-3}$	↗ [b]
aGI	0.997	$1.8 \cdot 10^{-5}$	0.992	$1.3 \cdot 10^{-6}$	↘
$\sqrt{aGI}$	0.999	$8.6 \cdot 10^{-7}$	0.991	$1.9 \cdot 10^{-6}$	↘

Table 3. Correlation parameters of dose gradient indices on the superficially averaged radius difference $\overline{\Delta r}_{\Delta D}(NT)\big|_{D_2}^{D_1}$ for nonspecific normal tissue (NT) according to Eq. (A.2) for the stereotactic radiotherapy of 25 choroidal melanomas. *r* - Pearson's correlation coefficient; *p* - probability of zero correlation; $\|\nabla \cdot D(\boldsymbol{r})\| \nearrow$ - increasing dose gradient magnitude; D_1 = 86% - level of the proximal isodose of interest relative to the nominal tumour dose 50 *Gy*; D_2 = 43% - level of the distal isodose of interest; ↗ - increasing dose gradient index; ↘ - decreasing dose gradient index; *GI* - dose gradient index according to Eq. (2); *DG* - dose gradient according to Eq. (A.8); *mGI* - modified dose gradient index according to Eq. (A.3); *aGI* - advanced dose gradient index according to Eq. (1); $\sqrt{aGI}$ - square root of the *aGI*. [a]Or the equivalent trend on $\overline{\Delta r}_{\Delta D}(NT)\big|_{D_2}^{D_1}$ ↘. [b]False trend compared to the intention of the dose gradient metric's authors.

Dose gradient index	***r* [1]**	***p* [1]**	**Trend on $\|\nabla \cdot D(\boldsymbol{r})\| \nearrow$ [a]**
GI	-0.511	$9.0 \cdot 10^{-3}$	↗ [b]
DG	0.496	$1.2 \cdot 10^{-2}$	↘ [b]
mGI	-0.444	$2.6 \cdot 10^{-2}$	↗ [b]
aGI	0.647	$4.7 \cdot 10^{-4}$	↘
$\sqrt{aGI}$	0.653	$4.0 \cdot 10^{-4}$	↘

3.6. Classification of advanced dose gradient index

Due to the definitions of the *aGI* and $\sqrt{aGI}$ according to Eq. (1), they are *a priori* implicit dose gradient measures in compliance with the classification scheme in Subsection 2.3; for details, see also [8]. From a mathematical point of view, an irrational algebraic function of a volume product is merely capable of indirectly describing dose gradients, but they can be called inversely proportional on the basis of the results in Subsection 3.5. The unit *cm* or $\sqrt{cm}$, respectively, is a further indication to a reciprocal dose gradient measure.

Moreover, both dose gradient indices showed true trends on a varying mean value of the physical dose gradients and did not over- or underestimate relative changes in physical dose gradients. Their dependencies on the target volume size were weaker than the overdependence of the *GI* on the target volume size. There will be no restrictions regarding comparisons of dose gradients, and the computational expense is little.

4. DISCUSSION

4.1. Trend reversal between *GI* and *aGI*

The curve characteristics of the input parameters required for the determination of the *GI*, *DG*, *mGI*, and *aGI* on a growing $x = d_{PTV}$ were analysed for the stereotactic radiosurgery of the brain metastases in Subsection 3.1. All of the functional dependencies could be adequately described by power functions of the type $f(x) = a \cdot x^b$. The author found that the two smaller volumes V_{PTV} and $V(D_1)$ grew faster on an increasing d_{PTV} than the larger one $V(D_2)$.

The false positive trends in the *GI*, *DG*, and *mGI* arise from this fact in combination with its definitions that contain ratios of the volumes of interest. Contrary to the authors' intention, the flatter the dose gradient, the smaller the values of the *GI* as well as *mGI* and the larger the value of the *DG*. As a result, the use of the *GI*, *DG*, or *mGI* regularly vexes medical physicists and radiotherapists. For example, the creators of the *GI* wrote: "... a *GI* of less than 3.0 generally reflects a reasonably selected prescription isodose level combined with a well-placed configuration of appropriately sized isocenters ... [4]".

The effect on a volume product and thus also on the values of the *aGI* is quite different: they ever increase on a decreasing magnitude of the physical dose gradients. Therefore, the steeper the physical dose gradient, the smaller the value of the *aGI;* the trends in the *aGI* become true negative.

4.2. Dependencies of dose gradient indices on target volume size at constant dose gradient

The parameter values $\Delta R = 3.0\ mm$ and $R_1 \in [1.5, 15.0]\ mm$ in the model calculations of Subsection 3.2 were realistically chosen on the basis of the corresponding parameters in the first irradiation series. The clinical superficially averaged radius differences and the clinical target volume radii were in ranges of 1.1 to 4.9 *mm* and 1.5 to 14.5 *mm*, respectively.

The ratio of the extremal functional values on the definition range, the extremal deviations of the functional values relative to the functional value at $R_1 = 7\ mm$, and the local derivative were determined for the *GI*, *aGI*, and $\sqrt{aGI}$. The dependency of the *GI* on the target volume radius was the strongest. The dose gradient index with the lowest dependency on the target volume size was $\sqrt{aGI}$ – regarding the first two criteria. The function course of an ideal dose gradient index would run parallel to the abscissa of Figure 2.

4.3. Functions of dose gradient indices on dose gradient

The input parameter values $R_1 \in [1.5, 15.0]\ mm$ and $c = R_2/R_1 = 3/2$ of the model calculations of Subsection 3.3 were realistically chosen on the basis of the corresponding parameters in both irradiation series. The clinical superficially averaged radii of the proximal isodoses at level D_1 and the clinical radius ratios c^* were in ranges of 1.5 to 14.6 *mm* and 1.3 to 1.8, respectively. Finally, the chosen constant c approximately was the centre of the total range of c^*. Consequently, the values of the third input parameter ΔR were in a range of 0.8 to 7.5 *mm*.

According to the results of the model calculations in Subsection 3.3 and Figure 3, the *GI* is a

completely indifferent dose gradient measure and therefore useless to quantify dose gradients. The *aGI* is an ideal dose gradient index that was directly proportional to the physical dose gradient described by ΔR.

Consequently the course of $\sqrt{aGI}$ was disproportionately low on a growing radius difference ΔR. In contrast, nearly linear functional relationships were presented in Figures 6 and 7. This apparent contradiction can be resolved by means of the results in Figure 4. Correspondingly, the square root of the proportionality factor in Eq. (6) is not constant, but a disproportionately high increasing function on $\bar{r}_1$ and $\Delta r_{\Delta D}(NT)|_{D_2}^{D_1}$. Therefore, the product of this function and the square root of the argument in Eq. (6) showed nearly linear curve characteristics on $\Delta r_{\Delta D}(NT)|_{D_2}^{D_1}$.

4.4. Curve characteristics of dose gradient measures on target volume size

A look at Figure 5 is not only useful to plausibility checks of the qualitative trends in the two-dimensional dose gradient measures on the target volume size in Subsection 3.4. The content of Figure 5 also consolidates the results in Subsection 3.1 and the statements in Subsection 4.1 that verify and describe, respectively, the false positive trends in the *GI*, *DG*, and *mGI* on a growing target volume size. Consequently, they overvalued the physical dose gradients – the basic problem of all of the dose gradient indices defined as volume ratios of the isodoses of interest.

Figure 5 shows true curve characteristics of the new dose gradient index *aGI* on d_{PTV} for both collimation types. To justify the choice of the reference quantity $\overline{\Delta r}_{\Delta D}(NT)|_{D_2}^{D_1}$ to find a more ideal dose gradient index than the *aGI*, the author postulated that the *aGI* is an inversely proportional dose gradient measure because of its unit *cm* and the proportionality in Eq. (6). From this point of view, the square root of the *aGI* is a nearly ideal dose gradient index in the first irradiation series.

The characteristics of the *aGI* shown in Figure 5 represent target curves for clinically acceptable values because the beam geometries were optimised to obtain the steepest possible isotropic dose gradients dependent on the target volume size. For other irradiation devices like Gamma Knifes® and CyberKnifes® ideal values of the *aGI* still have to be determined.

Careful readers surely would have noted that in Table 1 the coefficients and exponents of the regression functions for the dose gradient indices were not exactly consistent with those values that could be calculated by means of the power laws applied to the corresponding values for the volumes of interest. The reason was the chosen regression functions with $r^2 < 1$ – they are not perfect.

The discontinuities in the characteristic curves at $d_{PTV} = 14$ *mm* shown in Figures 1 and 5 were caused by the change in the collimation type. The physical penumbra of the 15 *mm* circular cone is distinctly smaller than that of the irradiation field aperture of the same size that is formed by the multi-leaf collimator. The unequal dose gradients are determined by different transmissions and geometries: The circular cone is a solid frustum manufactured from lead in contrast to the tungsten leafs with the finite isocentric width of 2.5 *mm*.

4.5. Correlation analyses between dose gradient measures

The trends of all of the dose gradient indices on an increasing reference variable were also examined by means of the results in Subsection 3.5.

The trends in the *aGI* and $\sqrt{aGI}$ on a decreasing magnitude of the physical dose gradients were true. The *GI*, *DG*, and *mGI* again showed false trends on $\overline{\Delta r}_{\Delta D}(NT)|_{D_2}^{D_1}$ as shown in Figures 6 and 7 and thus also false signs as shown in Tables 2 and 3. The regression lines shown in Figures 6 and 7 best fit the data series for the *aGI* and $\sqrt{aGI}$. The regression lines for the *DG* practically represented constant functions, though the *DG* showed stronger correlations than the *GI* and *mGI*; the standard deviations in the *GI* and *mGI* were obviously greater than that in the *DG*.

The slopes and ordinate intercepts of the regression lines for the *aGI* and $\sqrt{aGI}$ shown in Figures 6 and 7 were considerably different. The presented data do not substantiate a common and

universally valid scaling with the aim to obtain directly proportional regression lines of the special form $y = x$. At the moment, this special case seems to be an unattainable goal. Therefore, both dose gradient indices are not the same as a radius difference between the isodoses of interest, but they are proportional to it. The *aGI* and $\sqrt{aGI}$ can be regarded as reciprocal dose gradient measures. The trends in the *aGI* and $\sqrt{aGI}$ on the mean value of the physical dose gradients were almost linear in both clinical applications. The author will examine these relations in further irradiation series.

In the second irradiation series the author found nearly the same dependencies of the *aGI* and $\sqrt{aGI}$ on the target volume size than in the corresponding model calculation. The simple model is able to predict correctly this important property of dose gradient indices. For details and results, see Figure 2 as well as Subsections 2.4, 3.2, and 3.5.2.

4.6. Quality of dose gradient indices

The *aGI* and $\sqrt{aGI}$ were superior to the other assessed dose gradient indices *GI*, *DG*, and *mGI* with respect to the criteria

- realistic estimate of physical dose gradients with linear curve characteristics on the physical dose gradient;
- appreciable slope of the curve characteristics, which is quite different from zero, to prevent indifferent values;
- no restrictions regarding comparisons of dose gradients for different treatment techniques, irradiation modalities, patients, and irradiation series;
- independency on the target volume size at coincidently constant dose gradients.

A question to be answered is which of all of the assessed dose gradient indices describes best almost isotropic as well as anisotropic three-dimensional dose gradient problems. The square root of the *aGI* showed the best results in the

- model calculations concerning the dependency on the target volume size,
- correlation analyses for the stereotactic radiosurgery of the brain metastases, and
- correlation analyses for the stereotactic radiotherapy of the choroidal melanomas.

An ideal dose gradient index, which exactly describes relative variations of the dose gradients, should have characteristics between the limit functions $\sqrt{aGI}$ and *aGI*; for details, see the last paragraph of Subsection 3.4. The author recommends the *aGI* with its unit *cm* because the *aGI* is comparable with inversely proportional dose gradient measures that describe the dose gradient in the form of a radius difference with the unit *mm*.

Based on the statements in Subsection 4.5 and the findings in [8], it can be said that reciprocal and explicit dose gradient measures better describe anisotropic dose gradient distributions than the implicit ones. Two particularly suitable representatives of the first two categories are the one-dimensional metric $\Delta R_{1/2}$ [13] and the spatially averaged dose gradient $SADG^{*}|_{D_2}^{D_1}$ [15].

Wösle stated in [8] that both dose gradient indices best described the physical dose gradients in the first irradiation series for 13 brain metastases.

The clinical validity of correlations between the values of a dose gradient index and treatment complications has to be proved for all of the assessed dose gradient indices. The *aGI* and $\sqrt{aGI}$ have best prerequisites to pass these clinical tests through the fulfilments of the first three criteria mentioned in the first paragraph of this subsection.

A further open question is the suitability of the new *aGI* for the evaluation of treatment plans with non-stereotactic and irregularly formed target volumes. Investigations and results to this topic will be published in a separate article.

4.7. Revision of ICRU Report 91

The identified severe weaknesses of the recommended *GI* described in Section 3 were not mentioned in ICRU Report 91 [3] and in the review article [20]. A basis for discussion about better dose gradient indices than the widely used *GI* was presented in the form of Figure 5.

One aim of ICRU Report 91 was to better associate the gradient indices with treatment complications *via* rigorous and uniform reporting

of these parameters [3]. In this context, the *GI* is certainly not the first choice because the *GI* cannot be used to compare dose gradients at the boundary of planning target volumes of various sizes and in different irradiation series. As a consequence, Subsection *7.3 Reporting in SRT* of ICRU Report 91 concerning dose gradient metrics should be revised.

Instead of the *GI*, the author recommends the utilisation of the *aGI*, or alternatively of another reciprocal or explicit dose gradient index – at least as long as the algorithms of the more-dimensional dose gradient measures are not distributed.

4.8. Upgrade of treatment planning systems

The software developers of several systems for external beam planning have implemented the evaluation of the *GI* to display its value as a plan quality criterion. Due to the deficiencies of the *GI*, another dose gradient index is needed to support the aim of ICRU Report 91 specified in Subsection 4.7.

If the determination of the *aGI* or of one of the dose gradient indices specified in Subsection 4.6 was implemented in all of the existing treatment planning systems, the utilisation of dose gradient measures better than the *GI* would be easy for all users. There would be no additional computational expense.

5. CONCLUSION

The reason for false trends in dose gradient indices based on volume ratios of the isodoses of interest is the quotient in conjunction with differently increasing volumes of interest on a growing target volume size. Hence, the fundamental problems based on the severe deficiencies of the *GI*, *DG*, and *mGI* come from its definitions.

To rectify these serious problems, the author used functions of the product of the volumes of interest whereby a trend reversal has been accomplished. In this way, the new *aGI* became the best of all of the assessed dose gradient indices with respect to several quality criteria. The author showed that the *aGI* acts like a reciprocal dose gradient measure.

The utilisation of the *aGI* entails no limitations of the comparability of dose gradient values because the trends in the *aGI* are nearly linear on the physical dose gradient. The presented results suggest that the *aGI* is well endowed with good features to pass clinical validity tests concerning strong correlations between the severity of treatment complications and the values of the dose gradient index.

The worst of all of the dose gradient indices investigated in this article has been favoured in ICRU Report 91 for reporting in stereotactic radiotherapy. In doing so, it is hardly possible to fulfil the aim of better associating the dose gradient indices with treatment complications *via* reporting of these parameters. The subsection in ICRU Report 91 regarding reporting in stereotactic radiotherapy should be revised.

The common dose gradient indices like the *GI*, *DG*, and *mGI* are implicit dose gradient measures according to the classification scheme cited in Subsection 2.3. Their application makes it difficult for users to interpret the results and to infer the physical dose gradients from the results. As a consequence, the values of these dose gradient indices cannot be compared with basic data of the utilised irradiation device. Users are not able to comment on the absolute quality of the achieved results.

In contrast, the *aGI* nearly behaves like an inversely proportional dose gradient measure that has been shown through Eq. (6), without the aforementioned difficulties in application. The beam geometry described in Subsection 2.8.1 minimised both the anisotropy of the isodoses of interest and the values of $\overline{\Delta r}_{\Delta D}$. Therefore, the characteristics for the *aGI* shown in Figure 5 represent target curves for clinically acceptable values for the linac-based stereotactic radiosurgery and radiotherapy.

The author highly recommends the utilisation of the *aGI* – at least as long as the algorithms for the calculation of the more-dimensional dose gradient measures are not distributed. The *GI* and other dose gradient indices derived from it should no longer be used. All of the treatment planning systems that utilise the *GI* should be simultaneously upgraded with the revision of ICRU Report 91.

FUNDING

No funding at all has been claimed for this study.

ACKNOWLEDGEMENT

The author thanks Professor Ilja Frank Ciernik, head of department, for the provision of the utilised treatment planning system.

CONFLICT OF INTEREST STATEMENT

Markus Wösle declares that he has no competing interests.

APPENDIX

A.1. Superficially averaged dose gradient and superficially averaged radius difference

The mathematical formulations of the linearised two-dimensional anisotropic dose gradient problem for nonspecific normal tissue (*NT*) and an arbitrary organ at risk (OAR_i)

$$SADG\,(X)\,|_{D_2}^{D_1} = \frac{1}{\Omega_X}\cdot\int_{(\varphi_X)}\int_{(\vartheta_X)}\frac{D_2-D_1}{r_2(\varphi,\vartheta)-r_1(\varphi,\vartheta)}\cdot\sin\vartheta\cdot d\vartheta\cdot d\varphi\ \in\mathbb{R}^-,\quad X\in\{NT,OAR_i\} \tag{A.1}$$

are quotients of surface integrals of the difference quotient $\Delta D/\Delta r$ and solid angles. The underlying system of coordinates $\mathrm{K}=\{O,r,\varphi,\vartheta\}$ is defined by the origin *O* in the geometrical mass centre of the planning target volume and the three curvilinear coordinates: radius *r*, azimuth φ, and polar distance angle ϑ. Eq. (A.1) is the result of applying the generalised first mean value theorem for integration to the surface integrals [21].

The anisotropic radii r_1 and r_2 are the lengths of the position vectors to the surface points of the isodoses of interest. Their dose levels D_1 and D_2 define the surfaces of the treated and irradiated volumes, respectively. The surface element and solid angle element of the unit sphere are $dS=\sin\vartheta\cdot d\vartheta\cdot d\varphi=d\Omega$ with which the difference quotient must be integrated. For the normal tissue, the integration range is the entire solid angle $\Omega_{NT} = 4\cdot\pi\ sr$ with the angle ranges $\varphi_{NT} = [0, 2\cdot\pi]$ and $\vartheta_{NT}=[0,\pi]$. For each organ at risk, the individual segment Ω_{OAR_i} of the entire solid angle is defined by the angle ranges φ_{OAR_i} and ϑ_{OAR_i}. All of the needed input data are content of the structure file RS.*.dcm from the utilised treatment planning system [8].

The superficially averaged radius difference

$$\overline{\Delta r}_{\Delta D}\,(X)\,|_{D_2}^{D_1} = \frac{D_2-D_1}{SADG\,(X)\,|_{D_2}^{D_1}}\ \in\mathbb{R}^+,\quad X\in\{NT,OAR_i\} \tag{A.2}$$

is a result of applying the definition of the difference quotient $\Delta D/\Delta r = (D_2 - D_1)/\Delta r_{\Delta D}$ on the results of Eq. (A.1); it is itself a dose gradient measure of the category II according to Subsection 2.3 [8].

A.2. Common dose gradient indices

The explanations of abbreviations used more than once and quantities are provided at the beginning. The prescription isodose *PI*(*PTV*) and half the prescription isodose *PI*(*PTV*)/2 at the boundary of the planning target volume (PTV), the volume $V_{PI(PTV)}$ encompassed by *PI*(*PTV*), the volume $V_{PI(PTV)/2}$ encompassed by *PI*(*PTV*)/2, and the volume V_{PTV} of PTV.

The modified dose gradient index

$$mGI = \frac{V_{PI(PTV)/2}}{V_{PTV}} \tag{A.3}$$

derived from Eq. (2) was defined by Ohtakara *et al.* [7].

The unified dosimetry index

$$UDI = 10^4\cdot\prod_{k=1}^{4}[w_k\cdot(|1-DI_k|+0.1)]\ ,\quad w_1\cdot w_2\cdot w_3\cdot w_4 = 1 \tag{A.4}$$

of Akpati *et al.* combines the four dose indices

$$DI_1\equiv C=\frac{V_{PTV}\,(PI)}{V_{PTV}}\ , \tag{A.5}$$

$$DI_2\equiv CI=\frac{V_{PI(PTV)}}{V_{PTV}}\ , \tag{A.6}$$

$$DI_3 \equiv HI = \frac{D_{max}(PTV)}{D_{PI(PTV)}}\,, \tag{A.7}$$

$$DI_4 \equiv DG = \frac{V_{PI(PTV)}}{V_{PI(PTV)/2}} \tag{A.8}$$

to describe the dose coverage *C* of the planning target volume, the dose conformity *CI* of the prescription isodose with the shape and size of the planning target volume, the dose homogeneity *HI* within the planning target volume, and the dose gradient *DG*, respectively. The dose indices DI_k are weighted by the factors w_k, $k \in \{1, 2, 3, 4\}$. $V_{PTV}(PI)$ is the partial volume of the planning target volume receiving at least the dose $D_{PI(PTV)}$ of the prescription isodose. $D_{max}(PTV)$ is the maximum dose within the planning target volume. Eq. (A.8) is the reciprocal of Eq. (2) [9].

REFERENCES

1. Landberg, T., Chavaudra, J., Dobbs, J., Gerard, J. P., Hanks, G., Horiot, J. C., Johansson, K. A., Möller, T., Purdy, J., Suntharalingam, N. and Svensson, H. 1999, J. Int. Comm. Radiat. Units Meas., 32, 1.
2. International Commission on Radiation Units and Measurements. 2010, J. Int. Comm. Radiat. Units Meas., 10, 1.
3. International Commission on Radiation Units and Measurements. 2014, J. Int. Comm. Radiat. Units Meas., 14, 1.
4. Paddick, I. and Lippitz, B. 2006, J. Neurosurg. (Suppl.), 105, 194.
5. Flickinger, J. C., Kondziolka, D., Lunsford, L. D., Kassam, A., Phuong, L. K., Liščák, R. and Pollock, B. 2000, Int. J. Radiat. Oncol. Biol. Phys., 46, 1143.
6. Korytko, T., Radivoyevitch, T., Colussi, V., Wessels, B. W., Pillai, R., Maciunas, R. J. and Einstein, D. B. 2006, Int. J. Radiat. Oncol. Biol. Phys., 64, 419.
7. Ohtakara, K., Hayashi, S. and Hoshi, H. 2011, J. Radiat. Res., 52, 592.
8. Wösle, M. 2020, Z. Med. Phys., 30, 70.
9. Akpati, H., Kim, C. S., Kim, B., Park, T. and Meek, A. 2008, J. Appl. Clin. Med. Phys., 9, 99.
10. Liščák, R., Novotný, J., Urgošik, D., Vladyka, V. and Šimonová, G. 2000, Radiosurg., 3, 205.
11. Hellerbach, A., Luyken, K., Hoevels, M., Gierich, A., Rueß, D., Baus, W. W., Kocher, M., Ruge, M. I. and Treuer, H. 2017, Radiat. Oncol., 12, 136.
12. Sheth, N. S., Sim, S., Cheng, J., Lustgarten, J., Estin, D., Olson, T., Weiss, M., Murphy, S., Chen, Y. and Yang, J. 2011, Int. J. Radiat. Oncol. Biol. Phys., 81, S867.
13. Ruschin, M., Lee, Y., Beachey, D., Yeboah, C., Wronski, M., Babic, S., Lochray, F., Nico, A., Khan, L., Soliman, H. and Sahgal, A. 2016, Technol. Can. Res. Treat., 15, 130.
14. Sung, K. and Choi, Y. E. 2018, PLoS One, 13, e0196664.
15. Wösle, M., Krause, L., Sreenivasa, S., Vordermark, D. and Ciernik, I. F. 2018, Strahlenther. Onkol., 194, 929.
16. Wagner, T. H., Bova, F. J., Friedman, W. A., Buatti, J. M., Bouchet, L. G. and Meeks, S. L. 2003, Int. J. Radiat. Oncol. Biol. Phys., 57, 1141.
17. International Electrotechnical Commission. 2007, Medical electrical equipment – Medical electron accelerators – Functional performance characteristics (IEC 60976: 2007), VDE Verlag GmbH, Berlin.
18. Weiß, C. 2001, Basiswissen Medizinische Statistik, 2nd Ed., Springer-Verlag GmbH, Berlin, Heidelberg, New York.
19. Kocher, M., Wittig, A., Piroth, M. D., Treuer, H., Seegenschmiedt, H., Ruge, M., Grosu, A.-L. and Guckenberger, M. 2014, Strahlenther. Onkol., 190, 521.
20. Wilke, L., Andratschke, N., Blanck, O., Brunner, T. B., Combs, S. E., Grosu, A.-L., Moustakis, C., Schmitt, D., Baus, W. W. and Guckenberger, M. 2019, Strahlenther. Onkol., 195, 193.
21. Bronstein, I. N. and Semendjajew, K. A. 1987, Taschenbuch der Mathematik, 23rd Ed., Verlag Harri Deutsch, Thun, Frankfurt (Main).